Deterministic aperiodic arrays of metal nanoparticles for surface-enhanced Raman scattering (SERS)

Ashwin Gopinath[1], Svetlana V. Boriskina[1], Björn M. Reinhard[2], Luca Dal Negro[1,3*]

[1]*Department of Electrical and Computer Engineering & Photonics Center, Boston University, 8 Saint Mary's Street, Boston, MA, 02215*

[2]*Department of Chemistry, Boston University, 590 Commonwealth Avenue, Boston, MA, 02215*

[3]*Division of Materials Science and Engineering, Boston University*
15 Saint Mary's Street, Brookline, MA 02446, USA

[*]*Corresponding author: dalnegro@bu.edu*

Abstract: Deterministic Aperiodic (DA) arrays of gold (Au) nanoparticles are proposed as a novel approach for the engineering of reproducible surface enhanced Raman scattering (SERS) substrates. A set of DA and periodic arrays of cylindrical and triangular Au nanoparticles with diameters ranging between 50-110 nm and inter-particle separations between 25-100 nm were fabricated by e-beam lithography on quartz substrates. Using a molecular monolayer of pMA (p-mercaptoaniline) as a Raman reporter, we show that higher values of SERS enhancement factors can be achieved in DA structures compared to their periodic counterparts, and discuss the specific scaling rules of DA arrays with different morphologies. Electromagnetic field calculations based on the semi-analytical generalized Mie theory (GMT) fully support our findings and demonstrate the importance of morphology-dependent diffractive coupling (long-range interactions) for the engineering of the SERS response of DA arrays. Finally, we discuss optimization strategies based on the control of particles sizes and shapes, and we demonstrate that *spatially-averaged* SERS enhancement factors of the order of ~ 10^7 can be reproducibly obtained using DA arrays of Au nano-triangles. The ability to rigorously design lithographically fabricated DA arrays of metal nanoparticles enables the optimization and control of highly localized plasmonic fields for a variety of chip-scale devices, such as more reproducible SERS substrates, label-free bio-sensors and non-linear elements for nano-plasmonics.

OCIS codes: (240.6680) Surface plasmons; (240.6695) Surface-enhanced Raman scattering; (050.6624) Subwavelength structures; (290.4020) Mie theory.

References and links

1. M. Moskovits, "Surface-enhanced spectroscopy," Rev. Mod. Phys. **57**, 783-826 (1985).
2. K. A. Willets and R. P. Van Duyne, "Localized surface plasmon spectroscopy and sensing," Annu. Rev. Phys. Chem. **58**, 267-297 (2007).
3. Eds. K. Kneipp, M. Moskovits, and H. Kneipp, *Surface-Enhanced Raman Scattering* (Springer, Berlin, 2006).
4. Y. W. C. Cao, R. C. Jin, and C. A. Mirkin, "Nanoparticles with Raman spectroscopic fingerprints for DNA and RNA detection," Science, **297**, 1536-1540 (2002).
5. I. Delfino, A. R. Bizzarri, and S. Cannistraro, "Single-molecule detection of yeast cytochrome c by surface-enhanced Raman spectroscopy," Biophys. Chem. **113**, 41-51 (2005).
6. S. M. Nie and S. R. Emery, "Probing single molecules and single nanoparticles by surface-enhanced Raman scattering," Science, **275**, 1102-1106 (1997).
7. K. Kneipp, Y. Wang, H. Kneipp, L. T. Perelman, I. Itzkan, R. R. Dasari, and M. S. Feld, "Single molecule detection using surface-enhanced Raman scattering (SERS)," Phys. Rev. Lett. **78**, 1667-1670 (1997).

#106287 - $15.00 USD Received 13 Jan 2009; revised 3 Feb 2009; accepted 17 Feb 2009; published 25 Feb 2009

8. K. Kneipp, H. Kneipp, V. B. Kartha, R. Manoharan, G. Deinum, I. Itzkan, R. R. Dasari, and M. S. Feld, "Detection and identification of a single DNA base molecule using surface-enhanced Raman scattering (SERS)," Phys. Rev. E **57**, R6281-R6284 (1998).
9. D. R. Ward, N. K. Grady, C. S. Levin, N. J. Halas, Y. P. Wu, P. Nordlander, and D. Natelson, "Electromigrated nanoscale gaps for surface-enhanced Raman spectroscopy," Nano Lett. **7**, 1396-1400 (2007).
10. R. A. Tripp, R. A. Dluhy, and Y. Zhao, "Novel nanostructures for SERS biosensing," Nano Today **3**, 31-37 (2008).
11. R. M. Jarvis, A. Brooker, and R. Goodacre, "Surface-enhanced Raman scattering for the rapid discrimination of bacteria," Faraday Discuss. **132**, 281-292 (2006).
12. M. Fleischmann, P. J. Hendra, and A. J. McQuillan, "Raman spectra of pyridine adsorbed at a silver electrode," Chem. Phys. Lett. **26**, 163-166 (1974).
13. D. L. Jeanmaire and R. P. Van Duyne, "Surface Raman spectroelectrochemistry Part I. Heterocyclic, aromatic, and aliphatic amines adsorbed on the anodized silver electrode," J. Electroanal. Chem. **84**, 1-20 (1977).
14. C. V. Raman, "A change of wave-length in light scattering," Nature **121**, 619-619 (1928).
15. M. Kerker, D.-S. Wang, and H. Chew, "Surface enhanced Raman scattering (SERS) by molecules adsorbed at spherical particles," Appl. Opt. **19**, 3373-3388 (1980).
16. J. Gersten and A. Nitzan, "Electromagnetic theory of enhanced Raman scattering by molecules adsorbed on rough surfaces." J. Chem. Phys. **73**, 3023-3037 (1980).
17. F. J. García-Vidal and J. B. Pendry, "Collective theory for surface enhanced Raman scattering," Phys. Rev. Lett. **77**, 1163-1166 (1996).
18. E. C. Le Ru and P. G. Etchegoin, "Rigorous justification of the $|E|^4$ enhancement factor in Surface Enhanced Raman Spectroscopy," Chem. Phys. Lett. **423**, 63-66 (2006).
19. H. Xu, J. Aizpurua, M. Käll, and P. Apell, "Electromagnetic contributions to single-molecule sensitivity in surface-enhanced Raman scattering," Phys. Rev. E **62**, 4318-4324 (2000).
20. L. Gunnarsson, E.J. Bjerneld, H. Xu, S. Petronis, B. Kasemo, and M. Kall, "Interparticle coupling effects in nanofabricated substrates for surface-enhanced Raman scattering," Appl. Phys. Lett. **78**, 802-804 (2001).
21. Y.-J. Liu, Z.-Y. Zhang, Q. Zhao, and Y.-P. Zhao, "Revisiting the separation dependent surface enhanced Raman scattering," Appl. Phys. Lett. **93**, 173106 (2008).
22. C. E. Talley, J. B. Jackson, C. Oubre, N. K. Grady, C. W. Hollars, S. M. Lane, T. R. Huser, P. Nordlander, and N. J. Halas, "Surface-enhanced Raman scattering from individual Au nanoparticles and nanoparticle dimer substrates," Nano Lett. **5**, 1569-1574 (2005).
23. P. J. Schuck, D. P. Fromm, A. Sundaramurthy, G. S. Kino, and W. E. Moerner, "Improving the mismatch between light and nanoscale objects with gold bowtie nanoantennas," Phys. Rev. Lett. **94**, 017402 (2005).
24. M. Moskovits, L. L. Tay, J. Yang, and T. Haslett, "SERS and the single molecule," Top. Appl. Phys. **82**, 215-226 (2002).
25. A. Bek, R. Jansen, M. Ringler, S. Mayilo, T. A. Klar, and J. Feldmann, "Fluorescence enhancement in hot spots of AFM-designed gold nanoparticle sandwiches," Nano Lett. **8**, 485-490 (2008).
26. R. G. Freeman, K. G. Grabar, K. J. Allison, R. M. Bright, J. A. Davis, A. P. Guthrie, M. B. Hommer, M. A. Jackson, P. C. Smith, D. G. Walter, and M. J. Natan, "Self-assembled metal colloid monolayers: an approach to SERS substrates," Science **267**, 1629-1632 (1995).
27. S. J. Oldenburg, S. L. Westcott, R. D. Averitt, and N. J. Halas, "Surface enhanced Raman scattering in the near infrared using metal nanoshell substrates," J. Chem. Phys. **111**, 4729-4735 (1999).
28. J. B. Jackson and N. J. Halas, "Surface-enhanced Raman scattering on tunable plasmonic nanoparticle substrates," PNAS. **101**, 17930-17935 (2004).
29. Y. Lu, G.L. Liu, J. Kim, Y. X. Mejia, and L. P. Lee, "Nanophotonic crescent moon structures with sharp edge for ultrasensitive biomolecular detection by local electromagnetic field enhancement effect," Nano. Lett. **5**, 119-124 (2005).
30. V. Shalaev, *Optical Properties of Nanostructured Random Media* (Springer-Verlag, 2002).
31. Z. Wang, S. Pan, T. D. Krauss, H. Du, and L. J. Rothberg, "The structural basis for giant enhancement enabling single-molecule Raman scattering," PNAS. **100**, 8636-8643 (2003).
32. K. Li, M. I. Stockman, and D. J. Bergman, "Self-Similar chain of metal nanospheres as an efficient nanolens," Phys. Rev. Lett. **91**, 227402 (2003).
33. J. Dai, F. Cajko, I. Tsukerman, and M. I. Stockman, "Electrodynamic effects in plasmonic nanolenses," Phys. Rev. B **77**, 115419 (2008).
34. V. M. Shalaev and M. I. Stockman, "Optical properties of fractal clusters (susceptibility, surface enhanced Raman scattering by impurities)," Sov. Phys. JETP. **65**, 287-294 (1987).
35. X. Zhang, C. R. Yonzon, M. A. Young, D. A. Stuart, and R. P. Van Duyne, "Surface-enhanced Raman spectroscopy biosensors: excitation spectroscopy for optimisation of substrates fabricated by nanosphere lithography," IEE Proc.-Nanobiotechnol. **152**, 195-206 (2005).
36. H. Perry, A. Gopinath, D. L Kaplan, L. Dal Negro, and F. G. Omenetto, "Nano- and micropatterning of optically transparent, mechanically robust, biocompatible silk fibroin films," Advanced Mater. DOI: 10.1002/adma.200800011.

#106287 - $15.00 USD Received 13 Jan 2009; revised 3 Feb 2009; accepted 17 Feb 2009; published 25 Feb 2009

37. A. Wokaun, J. G. Bergman, J. P. Heritage, A. M. Glass, P. F. Liao, and D. H. Olson, "Surface second-harmonic generation from metal island films and microlithographic structures," Phys. Rev. B **24**, 849-856 (1981).
38. M. Kahl, E. Voges, S. Kostrewa, C. Vietz, and W. M. Hill, "Periodically structured metallic substrates for SERS," Sens. Actuators B. **51**, 285-291 (1995).
39. L. Gunnarsson, S. Petronis, B. Kasemo, H. Xu, J. Bjerneld, and M. Käll, "Optimizing nanofabricated substrates for Surface Enhanced Raman Scattering," Nanostruct. Mater. **12**, 783-788 (1999).
40. Q. Yu, P. Guan, D. Qin, G. Golden, and P. M. Wallace, "Inverted size-dependence of surface-enhanced Raman scattering on gold nanohole and nanodisk arrays," Nano Lett. **8**, 1923-1928 (2008).
41. N. Felidj, J. Aubard, G. Levi, J. R. Krenn, M. Salerno, G. Schider, B. Lamprecht, A. Leitner, and F. R. Aussenegg, "Controlling the optical response of regular arrays of gold particles for surface-enhanced Raman scattering," Phys. Rev. B, **65**, 075419 (2002).
42. L. Dal Negro, N. N. Feng, and A. Gopinath, "Electromagnetic coupling and plasmon localization in deterministic aperiodic arrays," J. Opt. A: Pure Appl. Opt. **10**, 064013 (2008).
43. A. Gopinath, S. V. Boriskina, N. N. Feng, B. M. Reinhard, and L. Dal Negro, "Photonic-plasmonic scattering resonances in determinsitic aperiodic structures," Nano Lett. **8**, 2423-2431 (2008).
44. R. Dallapiccola, A. Gopinath, F. Stellacci, and L. Dal Negro, "Quasi-periodic distribution of plasmon modes in two-dimensional Fibonacci arrays of metal nanoparticles," Opt. Express **16**, 5544-5555 (2008), http://www.opticsinfobase.org/oe/abstract.cfm?URI=oe-16-8-5544.
45. Y. L. Xu, "Electromagnetic scattering by an aggregate of spheres," Appl. Opt. **34**, 4573-4588 (1995).
46. B. Khlebtsov, A. Melnikov, V. Zharov, and N. Khlebtsov, "Absorption and scattering of light by a dimer of metal nanospheres: comparison of dipole and multipole approaches," Nanotechnol. **17**, 1437-1445 (2006).
47. S. Enoch, R. Quidant, and G. Badenes, "Optical sensing based on plasmon coupling in nanoparticle arrays," Opt. Express. **12**, 3422-3427 (2004), http://www.opticsinfobase.org/oe/abstract.cfm?URI=oe-12-15-3422.
48. B. Lamprecht, G. Schider, R. T. Lechner, H. Ditlbacher, J. R. Krenn, A. Leitner, and F. R. Aussenegg, "Metal nanoparticle gratings: influence of dipolar particle interaction on the plasmon resonance," Phys. Rev. Lett. **84**, 4721-4724 (2000).
49. S. Zou and G. C. Schatz, *Coupled plasmonic plasmon/photonic resonance effects in SERS* in Surface-(Enhanced Raman Scattering Springer, 2006).
50. N. Mohri, S. Matsushita, M. Inoue, and K. Yoshikawa, "Desorption of 4-Aminobenzenethiol bound to a gold surface," Langmuir. **14**, 2343-2347 (1998).
51. D. A. Genov, A. K. Sarychev, V. M. Shalaev, and A. Wei, "Resonant field enhancements from metal nanoparticle arrays," Nano Lett. **4**, 153-158 (2004).

1. Introduction

Surface-Enhanced Raman Scattering (SERS) spectroscopy is a well-established and highly sensitive technique for investigating the specific vibrational response of a variety of different analytes with fingerprinting accuracy. In particular, the SERS technique has been successfully applied to label-free chemical and biological sensing [1-3], where it has proven to be an excellent method for sensing DNA hybridization [4], protein binding events [5], and even single molecules [6-9]. In addition, it bears great promises for rapid identification of viruses and bacteria [10, 11], potentially enabling whole-organism fingerprinting.

Although the fundamental physics of SERS has been at the core of an intense debate since the pioneering works of Fleishman [12] in 1974 and Van Duyne [13] in 1977, it is now generally believed that the dramatic enhancement of the Raman scattering efficiency [14] observed in SERS experiments is mainly driven by the enhanced local electromagnetic fields in nanostructured metal surfaces [15-17]. In fact, despite SERS enhancement can also be affected by the specific electronic resonances (electronic enhancement) of Raman-active molecules and by their direct contact with metal surfaces (chemical enhancement), the dominant factor originates from a resonance effect between the incident and the scattered radiation fields associated to the excitation of surface plasmon resonances. In particular, it can be shown that the Raman enhancement scales roughly as the fourth power of the local field [1,16,17]:

$$G_{SERS} \propto \left\| \mathbf{E}_{loc}(\omega_{exc}) / \mathbf{E}_{inc}(\omega_{exc}) \right\|^4, \quad (1)$$

where $\mathbf{E}_{loc}(\omega_{exc})$ and $\mathbf{E}_{inc}(\omega_{exc})$ are the amplitudes of the local and incident electric fields, respectively, at the excitation frequency ω_{exc}. Although Eq. 1 is an approximation, which is

#106287 - $15.00 USD Received 13 Jan 2009; revised 3 Feb 2009; accepted 17 Feb 2009; published 25 Feb 2009

valid for Raman shifts smaller than the widths of the plasmonic resonances in metal nanostructures, and for the induced Raman dipoles aligned parallel to the electric field of the pump beam [18], in most practical cases, it provides a very useful guideline for estimating and comparing Raman enhancement values in nanostructures. Therefore, in SERS spectroscopy it is of crucial importance to develop systems of interacting metal nanostructures capable of producing high field enhancement with highly reproducible characteristics on controllable metal-dielectric substrates. Previous studies revealed that local electromagnetic fields can be dramatically enhanced in the junctions between closely separated particles, forming so-called electromagnetic "hot spots" [19-25]. Alternatively, individual nanoparticles deposited on planar substrates generate high Raman enhancements, which follow the plasmon resonance of individual particles [6, 26-29]. However, presently the best approaches to generate efficient SERS surfaces rely on random "roughening" of metal surfaces by etching or by colloidal synthesis of nanoparticles resulting in aggregates statistically described by fractal morphologies [8, 30, 31]. Based on the dipolar quasi-static approximation, Stockman et al [32-34] developed a comprehensive theory of SERS enhancement in fractal aggregates. The giant fluctuations of the local fields characteristic of self-similar (fractal) structures leads to an efficient transfer of excitations towards progressively smaller length scales of the aggregates where the electromagnetic enhancement reaches the 10^{12} level needed to observe single molecule SERS [6, 7, 24]. Fractal aggregates and rough metal surfaces led to successful applications in single molecule spectroscopy [8], but they lack reproducibility and simple engineering design rules for deterministic optimization. Raman enhancement factors of ~ 10^8 have been reported in Ag nanoparticle arrays fabricated by the nanosphere lithography [35]. However, nanosphere size dispersion and position randomness limit the reproducibility of this approach.

On the other hand, these approaches clearly demonstrate the importance of the morphology dependent "structural enhancement", which is typical for multi-scale complex systems where both electrodynamical interactions (diffractive modes) and electrostatic coupling (lightning rod effect) contribute to the overall enhancement. Despite the goal of developing reproducible SERS substrates by nano-lithographic techniques has been central since the discovery of the SERS effect in the 1970s [1, 13-15], a unifying approach towards engineered SERS substrates is still lacking, precluding so far the possibility to fabricate reliable sensors and diagnostic solutions based on SERS.

Electron beam lithography (EBL) is an ideal method for the fabrication of engineered SERS substrates. In addition, the main limitations of the EBL approach, resulting from the lack of cost and time effective schemes for device fabrication and scalability can be overcome by efficient nano-imprint techniques with nanometer resolution [36]. Following the pioneering work of Wokaun et al [37], it has been repeatedly demonstrated that SERS signals can be obtained from lithographically defined metal nanostructures [20, 21, 38-41], and Raman enhancement of 10^4-10^5 has been demonstrated. By using EBL it is possible to fabricate uniform SERS substrates by controlling both the shape and the position of each particle at the nanoscale. The SERS enhancement achievable using periodic arrays of metal nanoparticles can be further increased by reducing their inter-particle separations [20, 21]. However, the width of the inter-particle gaps achievable by EBL is limited to approximately 20 nm, which is much larger than the inter-particle separation obtained using random colloidal aggregates (1-5 nm). Therefore, in order to take full advantage of structural enhancement effects in highly reproducible EBL-based substrates, the subtle interplay between diffractive and near-field coupling in nanoparticles arrays with complex, yet deterministic, morphologies must be investigated and understood. It has recently been shown that by engineering the shapes of nanoparticles high values of field enhancement can be achieved [19], and hot-spot Raman enhancement factors >10^6 have been observed in the EBL-defined nanoscale gaps (20 nm) of bow-tie antennas [23].

In this paper, we propose the use of DA arrays of Au nanoparticles as a novel approach for the design and implementation of engineered SERS substrates with controllable hot-spots formation and large values (~ 10^7) of *average* enhancement factors in the arrays with the

#106287 - $15.00 USD Received 13 Jan 2009; revised 3 Feb 2009; accepted 17 Feb 2009; published 25 Feb 2009

minimum gaps of 25 nm. Recently, we demonstrated that far-field diffractive coupling is crucial to account for the broad plasmonic bands originating from photonic-plasmonic scattering resonances in deterministic aperiodic arrays of Au nanoparticles fabricated by EBL [42, 43]. In addition, we recently showed that the interplay between far-field electrodynamical and near-field quasi-static interactions in Fibonacci quasi-periodic arrays leads to larger values of hot-spots intensities, at predefined locations, with respect to periodic arrays of metal nanoparticles [44].

In the present paper, by combining experimental and rigorous electrodynamical calculations, we show that higher values of SERS enhancement can be achieved in DA structures compared to periodic systems. In addition, we discuss the specific engineering design rules for SERS enhancement in DA arrays and we demonstrate that ~ 10^7 SERS enhancement can be reproducibly achieved using DA arrays of nano-triangles.

2. Fabrication of deterministic aperiodic arrays

In order to systematically investigate the role of DA morphologies in the Raman enhancement of coupled arrays of Au nanoparticles, we have focused on the main exponents of deterministic aperiodic systems. These structures possess a very different degree of spatial complexity described by the spectral measures of their spatial Fourier spectra [42, 43]. In particular, we have studied periodic, quasi-periodic (Fibonacci), singular-continuous (Thue-Morse) and absolutely-continuous (Rudin-Shapiro) structures, which cover all the known classes of deterministic systems. Two-dimensional (2D) DA structures are generated by arranging identical nanoparticles in planar arrays according to symbolic inflation rules in two spatial dimensions [42, 43]. Unlike random structures, the positions of nanoparticles in DA arrays are uniquely specified once their minimum inter-particle separation has been chosen.

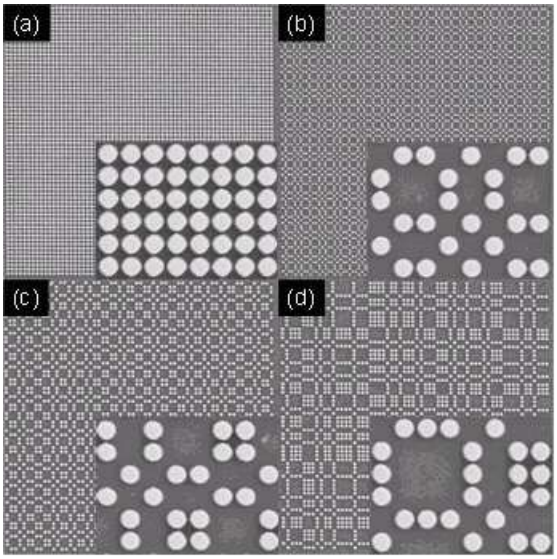

Fig. 1. Nanofabricated periodic (a), Fibonacci (b), Thue-Morse (c) and Rudin-Shapiro (d) arrays of Au nano-cylinders with 100 nm radii and 25 nm minimum edge-to-edge inter-particle separation.

All the Au nanoparticle arrays were fabricated using EBL on quartz substrates with a 10 nm layer Indium Tin Oxide (ITO) for conduction. A 180-nm-thick layer of PMMA (PolyMethylMethAcrylate) was spin coated on top of the cleaned substrate. Subsequently, the nanopatterning was defined using a Zeiss SUPRA 40VP SEM equipped with Raith Beam Blanker and nanometer pattern generation system (NPGS) with current and area dosage of 33.6pA and 400μC/cm^2 respectively. After developing the resist in a 1:3 solution of MIBK (Methyl IsoButyle Ketone) and IPA (Isopropanol), a 30-nm-thick Au film was deposited on

#106287 - $15.00 USD Received 13 Jan 2009; revised 3 Feb 2009; accepted 17 Feb 2009; published 25 Feb 2009

the patterned surface by electron-beam evaporation. Finally, a liftoff process was performed using Acetone, resulting in the designed Au nanoparticle arrays. Fig. 1 shows representative Scanning Electron Microscopy (SEM) images of fabricated DA arrays on quartz. The Au nanoparticles are cylindrical in shape with 200 nm diameter. Their height, which has been measured by Atomic Force Microscopy (AFM) and SEM, was found to be 30 nm. The minimum inter-particle separation for the specific structures shown in Fig. 1 is fixed to 25 nm. The dimensions of each fabricated array were 27 μm x 27 μm.

3. Computational analysis of hot spots formation and enhancement scaling

The main challenge for the engineering of more reproducible SERS substrates is identifying a geometrical configuration (morphology) of nanoparticles that leads, for a given choice of materials, sizes and shapes of nanoparticles, to the maximum field enhancement and concentration. Important aspects related to this question are the comparative study with respect to nanoparticles dimers, where intense hot-spots have been previously demonstrated [22-25], and the scaling of the enhancement with respect to the nanoparticles separations and the system's size.

In order to answer these questions, we first investigated the hot-spot formation in periodic and DA nanoparticle arrays by calculating the full electromagnetic field distributions in the array planes using the rigorous multi-particles Generalized Mie Theory [45]. Despite this approach can only be applied to spherical particles, it provides an analytical solution to the full Maxwell's equations, including retardation effects and all the necessary multipolar scattering orders, enabling the most accurate treatment of both the near-field and the far-field response of large nanoparticle arrays of arbitrary geometries [43]. It should also be noted that the ability to incorporate all multipolar orders in the electrodynamical interactions is crucial to account for the SERS enhancement of densely packed nanoparticles arrays. In fact, simpler but less accurate algorithms based on the retarded dipole approximation can fail to correctly reproduce the response of arrays composed of large (200 nm) and closely spaced (25 nm) nanoparticles like the ones considered in this paper [46]. However, since the fabricated arrays are composed of cylindrical and triangular shape nanoparticles as opposed to spherical ones, only the relative trends of the local fields for different arrays morphologies and dimensions, and not their absolute values, must be discussed within the idealized, yet rigorous, framework of GMT calculations.

Figure 2 shows a representative GMT calculation of the electric field distribution in periodic and DA arrays of Au nanoparticles with a diameter of 150 nm and a minimum separation of 25 nm. The numbers of particles in each array are indicated in the caption. All the arrays are uniformly excited by a plane wave at 785 nm, linearly polarized (horizontally) in the plane of the arrays. Localized surface plasmons, giving rise to hot-spot regions, are clearly visible for all the arrays within the gaps between nanoparticles. However, the field distribution in DA arrays reveals more complex patterns of field modulations induced by long-range multiple scattering (notice that the field patterns are plotted in logarithmic scale in order to better highlight the weaker long-range interactions). We will see in the next sections that these diffractive effects result in stronger enhancements at the hot-spots regions of DA arrays. We want to emphasize that, in contrast to the case of random colloidal aggregates, both the frequencies and the spatial locations of the hot-spots in DA arrays are uniquely determined by the morphology of the arrays. Based on Eq. (1) and the knowledge of the scattered fields, we can rigorously calculate the SERS enhancement and its scaling properties for different DA structures.

Figure 3 shows the maximum values of the GMT calculated Raman enhancement for arrays of various morphologies, inter-particle separations and numbers of particles. The case of a dimer of nanospheres is also shown for comparison. In Fig. 3(a), the Raman enhancement is plotted as a function of the nearest-neighbor separation for periodic and aperiodic arrays composed of ~100 nanospheres. It is interesting to notice that the results of the simulations for all the structures indicate a similar super-linear increase of the local field enhancement with decreasing inter-particle distance. The validity of this observation is also supported by

#106287 - $15.00 USD Received 13 Jan 2009; revised 3 Feb 2009; accepted 17 Feb 2009; published 25 Feb 2009

previous data on the scaling of Raman enhancement in single dimers [19, 25] and periodic arrays of nanoparticles with various shapes [20, 21]. However, Fig. 3(a) additionally demonstrates that the absolute value of the local fields responsible for the Raman enhancement is dramatically influenced by the arrays morphology. Our analytical GMT calculations on spherical nanoparticles indeed predict that periodic array yields the lowest enhancement compared to all DA arrays. This can be attributed to the more delocalized character of the plasmonic modes in periodic structures (see Fig. 2(a)), which is governed by long-range interactions of the surface plasmon resonances of individual nanoparticles [31]. Accordingly, our results also indicate that a single dimer structure provides a higher field enhancement than a large periodic array (Fig. 3(a)). This is in perfect agreement with previous observations that arrays composed of dimers outperform periodic arrays as optical sensing platforms based on stronger plasmon coupling [47]. It can also be observed in Fig. 3(a) that all the investigated aperiodic structures provide higher local field enhancement than either a periodic array or a nanoparticle dimer. It is important to notice that, even in the case of 100 nm inter-particle separation, the enhancement values are still drastically different for arrays of different morphologies and do not converge to the case of an isolated single-particle. This reflects the contribution of inter-particle coupling effects on local field enhancement [20, 21]. In fact, it has been already shown [48, 49] that even when particles are significantly separated so that near-field coupling can be neglected, the far-field interactions in deterministic nanoparticle arrays still dramatically influence the electromagnetic response through the formation of photonic-plasmonic resonances [43, 49].

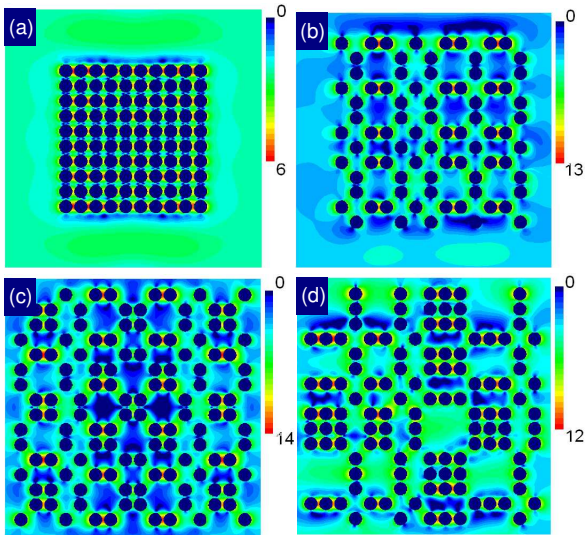

Fig. 2. Calculated electric field distributions in the plane of (a) periodic (b) Fibonacci, (c) Thue-Morse, and (d) Rudin-Shapiro second-generation arrays of gold nanospheres of 75 nm radii and 25 nm minimum inter-particle separation under the plane wave illumination at λ=785 nm with the E-field polarization parallel to the x-axis ($N^{per}=100$, $N^{Fib}=80$, $N^{TM}=128$, $N^{RS}=120$). The dispersion properties of Au nanoparticles are described using the Drude model with collision frequency of 250 THz, and plasma frequency of 6790 THz.

The scaling behavior of the Raman enhancement with respect to the number of nanoparticles in the arrays, at a fixed inter-particle separation of 50 nm, is shown in Fig. 3(b). The computational results shown in Fig. 3(b) reinforce the important role played by long-range diffractive coupling in DA arrays. In fact, we found that, for a fixed minimum interparticle separation, the local electric field in the hot spots (and thus the Raman signal) increases by increasing the number of particles. The Raman enhancement in the Fibonacci and Rudin-Shapiro structures grows almost linearly with the structure size. A more complex non-monotonic growth pattern is exhibited by the Thue-Morse structure and can be explained by

#106287 - $15.00 USD Received 13 Jan 2009; revised 3 Feb 2009; accepted 17 Feb 2009; published 25 Feb 2009

the distinctive inversion symmetry of the TM sequence, as demonstrated for one-dimensional Thue-Morse nanoparticle chains [42]. On the opposite side, periodic arrays do not give rise to an increase in the Raman enhancement with the increased structure size. These computational results indicate that the control of diffraction coupling and multiple scattering in complex DA arrays of metal nanoparticles offers the possibility to increase the hot-spots intensities by scaling the size of the systems, potentially providing orders of magnitudes larger enhancement with respect to isolated nanoparticle dimers.

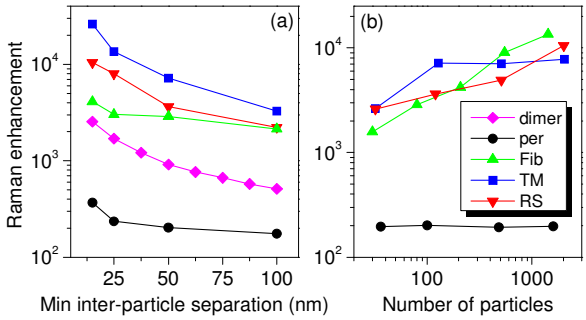

Fig. 3. Theoretically predicted Raman enhancement in arrays of Au nanoparticles of 100 nm radii with (a) varied minimum inter-particle separation ($N^{per}=100$, $N^{Fib}=80$, $N^{TM}=128$, $N^{RS}=120$) and (b) increased array sizes (minimum separation 50 nm).

The results shown in Fig. 3 clearly demonstrate that for DA arrays the in-plane long-range field interactions can reinforce the short-range quasi-static enhancement. This is a unique attribute of strongly fluctuating aperiodic environments, both DA or fractal structures. However, in the case of DA structures, it offers a unique opportunity for the engineering of controllable field enhancement and reproducible SERS substrates.

4. Experimental Raman spectra and enhancement factors

In this section, we discuss the experimentally measured SERS enhancement, and its intensity scaling, for periodic and DA arrays of cylindrical Au nanoparticles. Our engineered SERS substrates were cleaned in O_2 plasma for 10 min, rinsed in DI water and Acetone, dried with nitrogen flows, and immersed in a 10 μM aqueous solution of pMA (p-mercaptoaniline) for 1h in order to form a self-assembled monolayer of a Raman reporter on top of the nanoparticle arrays.

We used pMA as the Raman marker in this work because of its ability to form reproducible saturation coverage on gold surfaces [28, 50], which reduces the ambiguity associated with the experimental estimation of the Raman enhancement. Raman signal measurements were performed using a Renishaw Raman microscope (RM2000, Renishaw, IL). A 50× (N.A. = 0.55) objective was used to focus the laser beam on a nanostructured array and to collect the scattering light from the sample surface using a backscattering configuration. The SERS signal was acquired using 785 nm laser wavelength at 1.7mW excitation power. All SERS spectra were collected with a 10 s acquisition time. The dimension of the laser spot is constant (2.5 μm × 25 μm) ensuring that the SERS signal from the different arrays is comparable and unaffected by size variation.

Figsures 4 (a)-(d) show the Stokes Raman spectra of pMA molecular monolayers deposited on top of Au nano-cylinder arrays with different interparticle separations. The three dominant Stokes modes (390, 1077, 1590 cm^{-1}), arising from bending and stretching modes in the benzene rings of the pMA molecule [28], can clearly be distinguished in all the spectra. A broad background centered at 1400 cm^{-1} can also be observed, and it results from the quartz substrate. The intensity of the background signal varies for different arrays, in accordance with their respective filling fractions. In particular, the quartz background is more pronounced for DAS substrates because of their lower density of Au nanoparticles compared to periodic

#106287 - $15.00 USD Received 13 Jan 2009; revised 3 Feb 2009; accepted 17 Feb 2009; published 25 Feb 2009

arrays. We choose the 1077 cm^{-1} mode in order to extract quantitative information on the SERS enhancement and scaling for all the arrays. After background subtraction, the SERS enhancement factor for the 1077 cm^{-1} mode can be estimated from the experimental data by following the procedure discussed in [28]. The experimentally measured SERS enhancement is given by the ratio of Raman signal per molecule measured on the engineered substrates and the reference Raman signal per molecule originating from the pMA bulk crystal [28]:

$$G_{SERS} = RS_{EN} \times N_{REF} / RS_{REF} \times N_{EN} \ . \tag{2}$$

Here, RS_{EN} is the measured enhanced Raman signal from the nanoparticles arrays and and N_{EN} is the estimated number of molecules on the array which contribute to the measured signal.

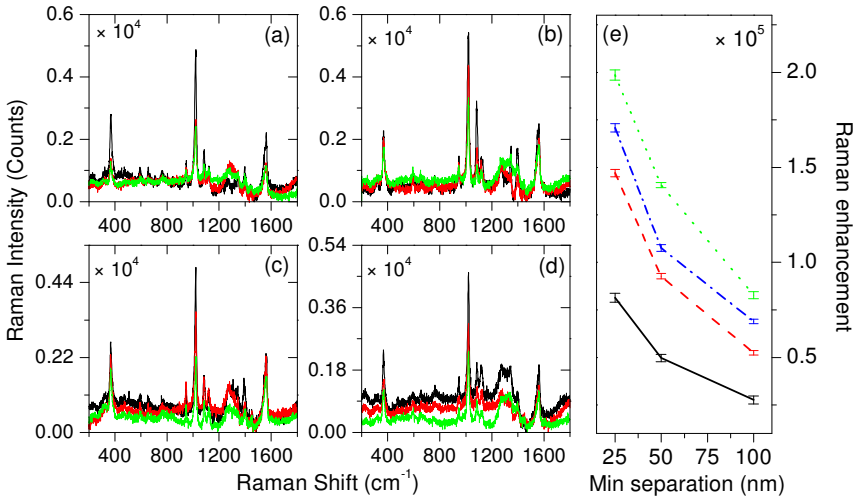

Fig. 4. Experimental Stokes SERS spectra of pMA on (a) Periodic, (b) Fibonacci, (c) Thue-Morse, and (d) Rudin-Shapiro arrays of Au nanocylinders with 100 nm radii and 25 nm (black), 50 nm (red), 100 nm (green) minimum inter-particle separation. (e) Enhancement factors calculated from the experimental data shown in (a)-(d) by using Eq. 2: Periodic (solid, black), Fibonacci (dot, green), Thue-Morse (dash-dot, blue), and Rudin-Shapiro (dash, red).

The number of molecules contributing to the SERS effect (N_{EN}) can be estimated as the ratio of the total gold surface illuminated by the laser beam and the geometrical cross section of the individual pMA molecules (0.3nm^2 per molecule) [50]. RS_{REF} and N_{REF} are the analogous quantities measured from the reference pMA sample in the absence of the SERS substrate. The latter quantity should now be calculated using the following formula:

$$N_{REF} = B_v \times D_{pMA} \times A / M_{pMA} \ , \tag{3}$$

where B_v is the optical excitation volume (2.5 μm × 25 μm × 5 μm), D_{pMA} is the density of pMA (1.06 g/cm^3) in the reference bulk crystal, A is the Avogadro number, and M_{pMA} is the molecular weight if pMA (125.19 AMU). The excitation volume was estimated as the product of the laser spot (2.5 μm × 25 μm) and the depth of focus $D_f \approx 2\lambda/(\mathrm{NA})^2$, where λ=785 nm is the excitation wavelength and NA=0.55 is the numerical aperture of the objective, thus yielding $D_f \approx 5$ μm.

It is important to notice that in our studies we can only access the average SERS enhancement over the broad distribution of enhancements present within the volume of the

#106287 - $15.00 USD Received 13 Jan 2009; revised 3 Feb 2009; accepted 17 Feb 2009; published 25 Feb 2009

SERS-active sample probed by the excitation beam. These experimental values are therefore to be considered as lower bounds for the hot-spot SERS enhancement in our chips.

The Raman enhancement factors at 1077 cm^{-1} calculated from the experimental spectra by using Eq. (2) are shown in Fig. 4(e) for arrays of different morphologies and interparticle separations. A strong super-linear growth of the Raman enhancement when decreasing the inter-particle distances is clearly observed for all the arrays, consistently with the simulation results shown in Fig. 3(a). Interestingly, we notice that different morphologies of the arrays result in different enhancement factors. In addition, all the DA arrays show larger enhancement factors compared to periodic arrays, for any given inter-particle separation.

It should be mentioned at this point that arrays of different morphologies exhibit scattering spectra centered at different wavelengths (see, e.g. Figs. 3 and 5 of Ref. 43 and Fig. 2 of Ref. 44), while the SERS data have been all collected at a fixed wavelength (785nm). In addition, we notice that the scattering spectra of periodic arrays of nano-cylinders spaced by 50-200 nm are blue-shifted with respect to the scattering peaks measured for DA arrays, but their peak positions shift to longer wavelengths when we increase the inter-particle separation [43]. When comparing the SERS factors of different structures, the spectral overlap between the excitation wavelength and the far-field scattering resonances is an important factor, although it should be noted that in particle aggregates the near-field spectra, which drive the SERS enhancement, can be distinctly different from the far-field ones, due to the onset of diffractive and multipolar scattering orders [3].

However, if we compare the experimentally measured SERS enhancement factors of periodic and DA arrays with overlapping scattering spectra peaked around the SERS excitation wavelength (785nm), we obtain almost an order of magnitude higher SERS enhancement for non-periodic structures, due a stronger field localization [3]. In particular, the measured SERS enhancement factor for a periodic array with 500 nm inter-particle separation, which strongly scatters at 735 nm (Fig. 3(a) of Ref. 43) is 8×10^3, while for a Fibonacci array with 100 nm minimum separation, which also scatters at the same wavelength, (Fig. 3(b) of Ref. 43), it is 7×10^4 (Fig. 4).

Therefore, our data demonstrate that aperiodic order has a strong effect in the SERS enhancement of DA arrays coupled in the diffractive regime, providing a novel strategy for the engineering of SERS substrates with morphology-dependent plasmonic resonances [43]. As a result, the engineering of multiply-scattering DA arrays is crucial to improve the performances of SERS substrates beyond the simple electrostatic description of nanoscale hot-spots. The importance and the contribution of fully electrodynamical interactions, such as diffractive photonic-plasmonic modes, in regular arrays of metal nanoparticles have only recently been discussed within a rigorous GMT approach [3, 43, 46].

Our experimental results on the SERS enhancement scaling in arrays of different sizes and morphologies are qualitatively supported by the semi-analytical GMT calculations shown in Fig. 3(a). In particular, all the aperiodic arrays give rise to higher SERS enhancement values compared to periodic arrays of the same interparticle distance, as predicted by GMT. However, as previously discussed, a direct quantitative comparison between GMT results and experimental data is not possible due to the non-spherical shape of the nanoparticles as well as their large number ($\sim10^5$), which precludes any rigorous GMT treatment. In particular, it is known [51] that the Raman enhancement obtained with nano-disks is approximately one order of magnitude larger than in the case of nanospheres, affecting the full electrodynamic coupling of the particles in the arrays. We believe that the non-spherical shape of the particles and the array sizes in our samples are at the origin of the minor discrepancies between our experimental data and the GMT calculations, which predicts the best enhancement for Rudin-Shapiro and Fibonacci structures.

5. Effect of nanoparticle size and shape

We will now investigate additional engineering strategies to further increase the Raman enhancement factors of deterministic SERS substrates. In particular, we will focus on tuning the size and the shape of the individual nanoparticles in arrays of different morphologies.

#106287 - $15.00 USD Received 13 Jan 2009; revised 3 Feb 2009; accepted 17 Feb 2009; published 25 Feb 2009

5.1. Enhancement scaling with nanoparticle radii

In this section, by combining GMT calculations and experimental data, we study the role of nanoparticle size on the Raman enhancement of periodic and DA nanoparticle arrays. For this purpose, a new set of samples was fabricated with particle sizes ranging in between 25 nm and 150 nm. All the arrays have a fixed minimum interparticle separation of 25 nm.

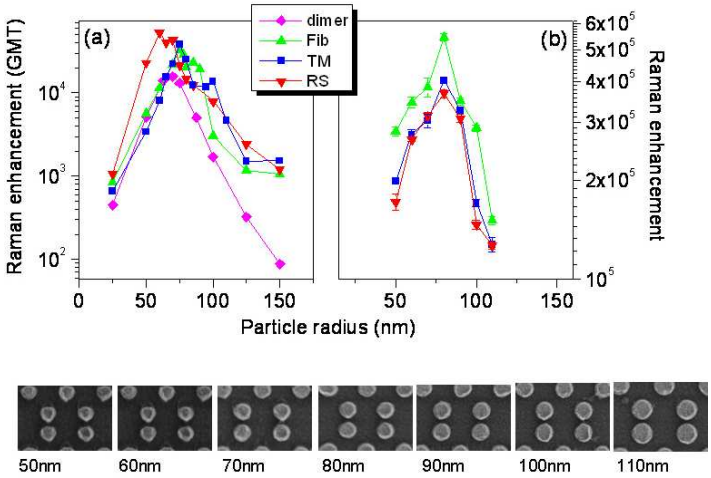

Fig. 5. Raman enhancement scaling with nanoparticle radii in arrays with minimum separation of 25 nm: (a) Theoretically predicted values for arrays of sizes $N^{per}=100$, $N^{Fib}=80$, $N^{TM}=128$, $N^{RS}=120$; (b) values derived from experimental data by using Eq. 2. The inset shows the SEM images of the nanofabricated arrays with nano-cylinders of different diameters.

The GMT results for all the arrays morphologies are plotted in Fig. 5(a), where we also show the SERS enhancement of a nanoparticle dimer for comparison. The results in Fig. 5(a) demonstrate that the performance of all the considered SERS arrays (including the dimer) can be improved by accurately tuning the particle radius. In addition, we note that arrays of different morphologies have different optimization radii, confirming the importance of the far-field coupling regime for the optimization of the near-field response of complex aperiodic arrays. The experimentally measured Raman enhancement factors for engineered arrays of different morphologies are shown in Fig. 5(b). The maximum SERS enhancement is displayed by arrays of nano-cylinders with 70-80 nm particle radii, which is in excellent agreement with the GMT predictions (Fig. 5(a)).

5.2. Raman enhancement in nano-triangle arrays

In this section we will consider the possibility to further improve the SERS enhancement of DA arrays by changing the shapes the individual nanoparticles. In particular, we will focus here on nano-triangular particles, which provide strong local fields around their sharp edges [19, 23]. The combined effects of tip-induced local field enhancement and far-field long-range coupling on DA morphologies have the potential to enable very sensitive SERS substrates within a perfectly engineerable approach. In order to investigate this effect experimentally, we fabricated periodic and DA arrays of Au nano-triangles with 200 nm side length, 30 nm thickness, and various inter-triangle separations. The SEM picture of nano-triangular arrays with 25 nm inter-particle separation is shown in Fig. 6. The radius of curvature of the tips of the nano-triangles is in the 17-20 nm range. The array fabrication process, the coating with pMA coating and the SERS measuring conditions were identical to the previously discussed case of arrays of nano-cylinders.

#106287 - $15.00 USD Received 13 Jan 2009; revised 3 Feb 2009; accepted 17 Feb 2009; published 25 Feb 2009

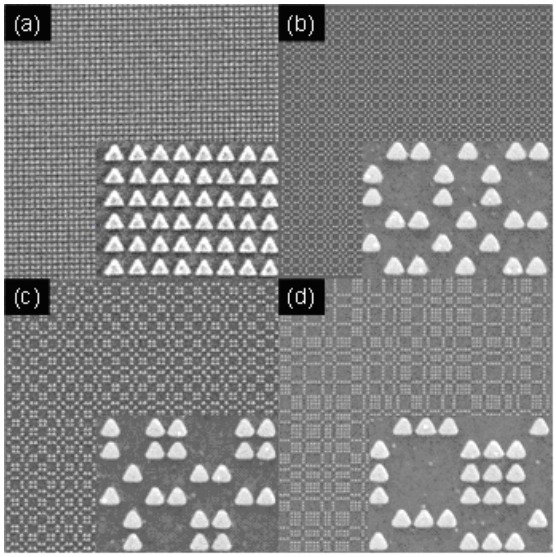

Fig. 6. Nanofabricated periodic (a), Fibonacci (b), Thue-Morse (c) and Rudin-Shapiro (d) arrays of Au equilateral nano-triangles with 200 nm side length and 25 nm minimum inter-particle separation.

In Figs. 7(a)-(d) we show the measured Raman signals from arrays of nano-triangles with different separations. The experimentally measured maximum Raman enhancement values (for the mode at 1077cm-^{1}) are shown in Fig. 7(e) for arrays of different morphologies and particle separations. Here, the spectra corresponding to different array separations are shifted upward for clarity. Our data demonstrate that the average SERS enhancement obtained with DA arrays of nano-triangles is almost two orders of magnitude larger than the one observed using nano-cylinder arrays (Fig. 4). However, it is important to notice that the scaling behavior of the morphology-dependent enhancement with the inter-particle distances is similar to the case of arrays of nano-spheres and nano-cylinders (see Figs. 7(e) and 4(e)). These results unambiguously demonstrate the fundamental role played by electrodynamical interactions (long-range diffractive coupling) in the local field enhancement observed within plasmonic nano-junctions. The maximum measured Raman enhancement in aperiodic nano-antennas with 25 nm minimum separation (Fig. 7(e)) is comparable with the record field enhancement values previously reported for arrays of bow-tie antennas with a smaller separation of 20 nm [23]. However, the state-of-the-art values ($G>10^{6}$) reported from lithographically defined bow-tie antennas correspond to the *local* hot-spot field intensity enhancement in the nano-gap region, as opposed to the *spatially averaged* values experimentally measured in our DA substrates. The highly inhomogeneous spatial distribution of the local hot-spots intensity predicted by rigorous simulations and demonstrated by NSOM data [44] manifest the full potential of aperiodic substrates for single molecule SERS detection based on deterministic designs. Moreover, the possibility to further optimize the SERS enhancement by carefully engineering the morphology of DA arrays offers a superior approach to reproducible create giant electromagnetic fields at the nanoscale. Our experimental findings show that the control of plasmonic hot-spots in complex DA arrays coupled by diffractive interactions provides a novel approach for the design and engineering of reproducible SERS chips with single-molecule sensitivity.

#106287 - $15.00 USD Received 13 Jan 2009; revised 3 Feb 2009; accepted 17 Feb 2009; published 25 Feb 2009

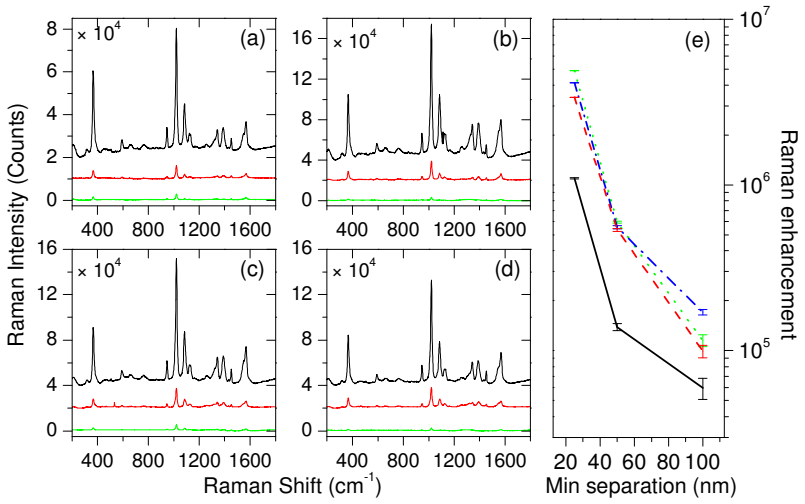

Fig. 7. Experimental Stokes SERS spectra of pMA on (a) Periodic, (b) Fibonacci, (c) Thue-Morse, and (d) Rudin-Shapiro arrays of Au nano-triangles with 200 nm side lengths and 25 nm (black), 50 nm (red), 100 nm (green) minimum inter-particle separation. (e) Enhancement factors calculated from the experimental data shown in (a)-(d) by using Eq. 2: Periodic (solid, black), Fibonacci (dot, green), Thue-Morse (dash-dot, blue), and Rudin-Shapiro (dash, red).

6. Conclusions

In this work, by combining accurate electrodynamical calculations and experimental data, we have demonstrated ~10^7 *average* SERS enhancement in lithographically defined DA arrays of Au nanoparticles. In particular, we clarified the fundamental role played by long-range diffractive coupling in the formation and intensity of local hot-spots, and we discussed the engineering scaling rules for DA arrays with different degrees of complexity. Our results show that larger enhancement factors with respect to individual particle dimers or periodic nanoparticle arrays can be achieved using carefully designed DA arrays with optimized morphology and particles' size. The ability to rigorously design and lithographically fabricate DA arrays of metal nanoparticles provides a novel approach for the engineering and optimization of reproducible SERS substrates and novel active components for nanoplasmonics applications.

Acknowledgments

The authors thank Prof. Enrico Bellotti for the opportunity to utilize the computational resources available in his laboratory at Boston University, Prof. Lawrence D. Ziegler for stimulating discussions on the SERS effect and Dr. Ranjith Premasiri for technical help with Raman characterization at Boston University. In addition, we would like to thank Y.-L. Xu and M. Ringler for making their Fortran codes available for public use. This work was partially supported by the US Army Research Laboratory under the contract numbers W911NF-06-2-0040, and W911 NF-07-1-0618.

#106287 - $15.00 USD Received 13 Jan 2009; revised 3 Feb 2009; accepted 17 Feb 2009; published 25 Feb 2009